PCCP

Accepted Manuscript

ROYAL SOCIETY OF CHEMISTRY

www.rsc.org/pccp

PCCP

RSCPublishing

ARTICLE

Adsorption and corrosion inhibition effect of Schiff base molecules on the mild steel surface in 1 M HCl medium: A combined experimental and theoretical approach

Cite this: DOI: 10.1039/x0xx00000x

Received 00th January 2012,
Accepted 00th January 2012

DOI: 10.1039/x0xx00000x

www.rsc.org/

Sourav Kr. Saha,[ab] Alokdut Dutta,[c] Pritam Ghosh,[a] Dipankar Sukul[c] and Priyabrata Banerjee[ab]*

Corrosion inhibition performance of 2-(2-hydroxybenzylideneamino)phenol (L^1), 2-(5-chloro-2-hydroxybenzylideneamino)phenol (L^2) and 2-(2-hydroxy-5-nitrobenzylideneamino)phenol (L^3) on the corrosion behaviour of mild steel surface in 1 M hydrochloric acid (HCl) solution are investigated by sophisticated analytical methods like potentiodynamic polarization, electrochemical impedance spectroscopy and weight loss measurements. Polarization studies showed that all the compounds are mixed type (cathodic and anodic) inhibitors and inhibition efficiency ($\eta_{\%}$) increased with increasing inhibitor concentration. The inhibition actions of these Schiff base molecules are discussed in view of blocking the electrode surface by means of adsorption of inhibitor molecule obeying Langmuir adsorption isotherm. Scanning electron microscopy (SEM) studies of the metal surfaces confirmed the existence of an adsorbed film. Density functional theory (DFT) and Molecular dynamics (MD) simulation have been used to determine the relationship between molecular configuration and their inhibition efficiencies. Order of inhibition performance obtained from experimental results is successfully verified by DFT and Molecular dynamics simulation.

Introduction

In several industrial processes hydrochloric acid solution is widely used as an acid wash solution (cleaning, pickling, descaling) for removing rust and scale from mild steel surface.[1-3] This usually leads to serious metallic corrosion. To prevent their aggressiveness, use of an additive is the most effective and sensible approach to protect several metal and alloys against such type of acidic attack.[4-5] A variety of additives are now a days used to prevent the metallic corrosion. In this connection, organic compounds containing electron rich functional groups along with π-electrons inside their frameworks shows better corrosion inhibition efficiency in such acid media. Till date the existing results show that, organic inhibitors adsorbed on the metallic surface either by physical or chemical adsorption or by both and eventually a protective layer is formed. Organic molecules having (i) N, O and S donor sites, (ii) unsaturated π-bonds, (iii) planar and conjugated aromatic rings are considered as effective adsorption centers, because of their capability to donate available lone pair of electrons or acceptance of electrons in their low energy empty orbitals.[6-9] Thus compounds containing both nitrogen (N) and oxygen (O) in their structural unit exhibits greater inhibition performance compare to those possessing only one of these heteroatoms.[10-12]

[a]*Surface Engineering & Tribology Group, CSIR-Central Mechanical Engineering Research Institute, Mahatma Gandhi Avenue, Durgapur 713209, West Bengal, India.*
E-mail: pr_banerjee@cmeri.res.in; Fax: +91-343-2546 745; Tel: +91-343-6452220
[b]*Academy of Scientific & Innovative Research, Anusandhan Bhawan, 2 Rafi Marg, New Delhi 110001, India*
[c]*Department of Chemistry, National Institute of Technology, Durgapur 713 209, India*

In these circumstances, researchers are mainly motivated for developing several new cost effective and easy to make organic compounds with adequate number of heteroatoms in their backbone. In literature out of several organic compounds, Schiff base compounds have been reported as effective corrosion inhibitors for metals and alloys in the acidic media.[13,14] Increasing popularity of Schiff bases in the field of material science are due to its low cost starting materials, relatively easy to undergo synthetic route, high purity, low toxicity and eco-friendly natures.[15-17] These facts motivate us towards the selection of three Schiff base molecules namely 2-(2-hydroxybenzylideneamino)phenol (L^1), 2-(5-chloro-2-hydroxybenzylideneamino)phenol (L^2) and 2-(2-hydroxy-5-nitrobenzylideneamino)phenol (L^3) as corrosion inhibitors. The choices of these molecules are also based on their structural considerations. These Schiff base molecules are consist of two benzene rings with delocalised π–electrons with electron rich substituent $–NO_2$, –Cl, –OH groups. This structural feature favours better interaction with the mild steel surface. In view of the above we have been chosen L^1, L^2 and L^3 for this present work.
Traditionally, scientists have identified new corrosion inhibitors following hardcore synthetic laboratory methods, which is laborious, expensive, time consuming and unable to reveal microcosmic inhibition process.[18,19] It becomes necessary to find out an alternative route where we can predict which molecule behaves as a good corrosion inhibitor and which are not. In view of above, computer simulation [*e.g.;* Density Functional Theory (DFT) and Molecular dynamics (MD) simulation] is the most authentic technique which has enormous advantages of evaluating microcosmic inhibition performance and exploration of their mechanism.[20,21] In our recent works, we have successfully investigated the corrosion inhibition

effectiveness of pyrazine derivatives,[22] marcapto-quinoline Schiff bases[23] by MD simulation and quantum chemical calculations. Results obtained from these studies have shed more light into the reactivity, active sites and the mechanism of interaction of these inhibitors with steel surface. These findings help us for rational designing of promising corrosion inhibitors.

The aim of this present work is to develop a bridging in-between the experimental and theoretical corrosion inhibition world to provide more insight fullness in view of the mechanism of inhibition action of the corrosion inhibitors. To do that, the first and foremost duty is to investigate the inhibition effectiveness of three Schiff base compounds against mild steel corrosion in hydrochloric acid medium by wet chemicals experimentation. Potentiodynamic polarization, electrochemical impedance spectroscopy and weight loss measurements are used to obtain the inhibition efficiency. Quantum chemical calculation and MD simulations are performed to investigate their relative corrosion inhibition performance from theoretical point of view. Several Quantum chemical properties like electronegativity (χ), softness (S), fraction of electron transfers from inhibitor to metal surface (ΔN) along with energy gap (ΔE) *etc* coming out from E_{HOMO}, E_{LUMO} are hereby studied. Local reactive sites of the present molecules have been analyzed through Fukui indices. Moreover, adsorption behaviour of the inhibitor molecules on Fe (1 1 0) surface have been analysed using MD simulation.

Experimental details

Materials

All the solvents and chemicals used for synthesis are of analytical grade. 2-amino phenol, 2-hydroxybenzaldehyde, 5-chloro-2-hydroxybenzaldehyde, 2-hydroxy-5-nitrobenzaldehyde are purchased from Spectrochem and used without doing further purification. 35% HCl (GR grade) is purchased from Merck India. Analytical grade methanol and ether are purchased from Fluka and used without any further purification.

Instrumentation

A Perkin Elmer 2400C elemental analyser was used to collect the microanalytical (C, H, N) data. IR spectra were carried out in a Perkin Elmer FT-IR spectrometer (spectrum 100) (Using KBr pellets). Melting point was measured under NICS-96. ESI-MS mass spectra were recorded on an Advion make compact mass spectrometer (Serial No: 3013-0140). Potentiodynamic polarization and electrochemical impedance measurements were carried out using Gill AC, ACM Instruments, UK. The morphology of corroded mild steel surface in presence and absence of inhibitor molecules was examined by a scanning electron microscopy (SEM) using Hitachi S-3000N, Japan instrument.

Synthesis of inhibitors

The Schiff base inhibitors are synthesized by a simple condensation reaction between equimolar amounts of 2-amino phenol and corresponding aldehydes (2-hydroxybenzaldehyde, 5-chloro-2-hydroxybenzaldehyde and 2-hydroxy-5-nitrobenzaldehyde) in methanolic medium. The excess methanol was evaporated under vacuum and the final product was washed twice with ether and finally dried in air. The structures of these molecules were confirmed by elemental analysis, ESI-MS and FTIR spectroscopy. The schematic presentation of molecular structures of L^1, L^2 and L^3 were shown in Fig. 1.

For L^1 ($C_{13}H_{11}NO_2$). Yield: 89%. Elemental Analysis: Anal. Cald.: C, 73.23; H, 5.20; N, 6.57. Found: C, 73.15; H, 5.13; N, 6.48%. M.P. = 187°. Characteristic IR peaks (KBr disk): υ_{O-H} = 3445,[24] υ_{C-H} = 3085,[25] $\upsilon_{C=N}$ = 1630,[26] $\upsilon_{C=C}$ = 1460,[27] υ_{C-O} = 1225 cm^{-1} [28] (Fig. S1). ESI-MS (L^1–H^+): 212.3 amu (Fig. S4).

For L^2 ($C_{13}H_{10}NO_2Cl$). Yield: 92%. Elemental Analysis: Anal. Cald.: C, 63.04; H, 4.07; N, 5.66. Found: C, 62.93; H, 4.01; N, 5.57%. M.P. = 52.5°. Characteristic IR peaks (KBr disk): υ(O-H) = 3430,[24] υ_{C-H} = 3070,[29] $\upsilon_{C=N}$ = 1620,[26] $\upsilon_{C=C}$ = 1445,[27] υ_{C-O} = 1220 cm^{-1} [28] (Fig. S2). ESI-MS (L^2–H^+): 246.2 amu (Fig. S5).

For L^3 ($C_{13}H_{10}N_2O_4$). Yield: 94%. Elemental Analysis: Anal. Cald.: C, 60.47; H, 3. 90; N, 10.85. Found: C, 60.34; H, 3.82; N, 10.74%. M.P. = 239.5°. Characteristic IR peaks (KBr disk): υ_{O-H} = 3425,[24] υ_{C-H} = 3065,[29] $\upsilon_{C=N}$ = 1615,[26] $\upsilon_{C=C}$ = 1540,[27] υ(Ph-NO_2) = 1325,[29] υ_{C-O} = 1200 cm^{-1} [28] (Fig. S3). ESI-MS (L^3–H^+): 257.1 amu (Fig. S6).

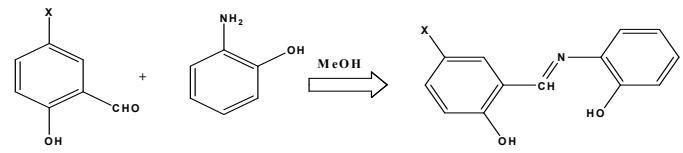

X	Abbreviation
H	L^1
Cl	L^2
NO_2	L^3

Fig. 1 Synthesis route and general structures of investigated Schiff bases.

Specimens and solution

Cylindrical specimens were prepared by cutting commercially available mild steel rod [Composition (wt%): 0.22 C, 0.31 Si, 0.60 Mn, 0.04 P, 0.06 S and Fe (remainder)]. Prior to each and individual experiment, the surfaces were pre-treated by grinding with belt grinding polishing machine followed by metallurgical grade (400-1600) emery papers. Afterwards the samples are degreased with ethanol and rinsed with double-distilled water (thrice). 1 M HCl solution was prepared using 35% HCl (GR grade, Merck India).

Electrochemical measurements

Potentiodynamic polarization and electrochemical impedance measurements were carried out using a conventional three electrode cell system. Mild steel was used as a working electrode (WE) with exposed surface area of 0.25 sq cm, in this electrochemical study counter and reference electrode was platinum sheet and SCE (saturated calomel electrode). Before measurements, the WE was kept in contact with test solution for 45 minutes to achieve a steady state. Polarization curve measurements were carried out at a scan rate of 0.5 mV/sec. Determination of corrosion current density (i_{corr}) was found from the intercept of the extrapolated cathodic and anodic Tafel lines at the corrosion potential (E_{corr}). Impedance spectroscopy experimentation were executed within the frequency range of 10 mHz to 100 kHz with a.c. amplitude of ± 10 mV (r.m.s.) at the open circuit potential (OCP). All the experiments were done at room temperature (~27°C).

Weight loss measurements

Weight loss measurement of polished mild steel rectangular coupons (2.5 x 2.5 x 0.1 cm^3) (wt% composition: 0.19 C, 0.21 Si, 0.21 Mn,

0.01 P, 0.01 S and the remainder iron) in 1 M HCl medium in absence and presence of different inhibitors were carried out at room temperature around 27°C. Mild steel coupons were immersed in 100 ml of 1 M HCl with and without three inhibitors [*e.g.;* L^1, L^2 and L^3 (5mM each)] for duration of 1 hour to 96 hour. Before immersion in acid solution, weights of the polished, cleaned and dried specimens were measured. After a fixed interval of experimental investigation all the specimens were taken out, washed thoroughly with distilled water to remove the corrosion product, dried with a hot air stream and calculated out the weight loss. Percentage of inhibition efficiency, $\eta_{\%w}$ was calculated at different time interval by the following formula:

$$\eta_{\%w} = \frac{w_0 - w}{w_0} \times 100 \quad (1)$$

Where, W_0 and W are the weight loss of mild steel specimens in acid solution with and without inhibitor for same immersion time. In each case, experiments were conducted thrice which shows that the results obtained were within ± 1% of the first.

Surface analysis

For morphological studies, mild steel specimens was prepared by keeping the samples in 1 M HCl medium with and without the organic inhibitors for duration of 6 h. The specimens were then washed gently with acetone followed by distilled water, after those carefully dried specimens were analyzed under SEM. Micrographs of all corroded specimens have magnification of ×200 to present a constant view.

Computational studies

Quantum chemical calculation

Quantum chemical method was performed to explore the correlation between molecular properties of the studied inhibitors in line with its corresponding inhibition efficiency. From a computational point of view DFT (Density Functional Theory) methods have become popular from the last few decades for their accuracy in respective calculation in lesser time with a much less investment. In this present study DFT calculations were performed with the ORCA programme package (version 2.7.0),[30] which is an open source code developed by Prof. Dr. Franc Neese (Director, MPI für Chemische Energiekonversion, Muelheim, Germany). Geometry optimizations of the compounds were done by using B3LYP.[31-36] Ahlrichs group has developed the all-electron Gaussian basis sets.[37] Herein, triple-ζ quality basis sets TZV(P) along with polarization function set on the N, O and Cl like atoms are used.[38] For atoms like carbon and hydrogen, we have used polarized split-valence SV(P) basis sets. Notably, in the valence region these were of double-ζ quality and on the nonhydrogen atoms those had a polarizing set of d functions. Self consistent field (SCF) calculations were converged [with 10^{-8} Eh : energy, 10^{-7} Eh : density change, 10^{-7} : maximum element of the DIIS (Direct Inversion in the Iterative Subspace or Direct Inversion of the Iterative Subspace) error vector]. All the theoretical parameters were calculated in the liquid phase because it is well known that the electrochemical corrosion always appears in liquid phase. As a result, it is necessary to include the effect of a solvent in the methodology of computational calculations. This was used for modelling the water as a continuum of uniform dielectric constant (ε) and the solute was placed as a uniform series of inlocking atomic spheres.

Reactive sites of the molecule has been analyzed by evaluating Fukui indices (FI). The FI calculation was performed using Dmol^3 module, Material studio^{TM} version 6.1 by Accelrys Inc, San Diego, CA.[39] All the calculations were performed using double numerical polarization (DNP) basis set (which includes both d and p orbital polarization functional) in combination with generalized gradient approximation (GGA) and Becke-Lee-Yang-Parr (BLYP) exchange-correlation functionals.[40,41] Detail information of local reactivity has been obtained by condensed Fukui functions.[42] The Fukui function f_k was defined as the first derivative of the electronic density $\rho(\vec{r})$ with respect to the number of electrons N in a constant external potential $\upsilon(\vec{r})$.[43]

$$f_k = \left(\frac{\partial \rho(\vec{r})}{\partial N} \right)_{\upsilon(\vec{r})} \quad (2)$$

For an electron transfer reaction, fukui function enlighten the sites in a molecule where nucleophilic, electrophilic or radical attacks are mostly possible. The Fukui functions has been written by taking the finite difference approximations as:[44]

$$f_k^+ = q_k(N+1) - q_k(N) \quad \text{(for nucleophilic attack)} \quad (3)$$

$$f_k^- = q_k(N) - q_k(N-1) \quad \text{(for electrophilic attack)} \quad (4)$$

$$f_k^0 = \frac{q_k(N+1) - q_k(N-1)}{2} \quad \text{(for radical based attack)} \quad (5)$$

Table 1 Electrochemical parameters obtained from Potentiodynamic Polarisation curves of mild steel in 1 M HCl solution with and without the various concentrations of Schiff bases at 27^0C

System	Conc (mM)	$-E_{corr}$ (mV per SCE)	i_{corr} (μA cm^{-2})	β_a (mVdec^{-1})	β_c (mVdec^{-1})	$\eta_{\%P}$
HCl	Blank	492	1200	79	102	—
L^1	0.1	491	971	83	107	19
	0.5	511	867	82	102	28
	1	503	742	86	110	38
	5	516	664	86	110	45
L^2	0.1	492	676	87	135	44
	0.5	499	502	85	116	58
	1	512	399	89	112	66
	5	507	297	82	114	75
L^3	0.1	504	642	94	108	47
	0.5	526	475	78	105	60
	1	507	378	80	100	69
	5	533	246	72	110	80

where q_k was the gross charge of k atom *i.e.;* the electronic density at a point r in space around the molecule. The q_k (N+1), q_k (N) and q_k (N-1) are defined as the charge of the anionic, neutral and cationic species respectively. Here Fukui functions were presented through the finite difference approximation using Hirshfeld population analysis (HPA).[45]

Molecular dynamics simulation

MD simulation is very popular for the investigation regarding interaction between the inhibitor molecule and the concerned metal surface. The interaction between inhibitors and iron (Fe) surface was investigated by MD simulation using Material Studio™ software 6.1 (from Accelrys Inc.).[39] Herein, we had chosen Fe (1 1 0) surface for simulation. Among other optional Fe surfaces [*e.g.*; Fe (1 0 0), Fe (1 1 1) *etc.*], Fe (1 1 0) surface was picked up for its packed surface and better stabilization.[46] The interaction between Fe (1 1 0) surface and studied inhibitors had been executed in a simulation box size of (32.27 × 32.27 × 70.26 Å) with periodic boundary conditions. A 50 Å height vacuum slab was introduced on the Fe (1 1 0) surface. The quantity of layers was chosen in such a way that surface depth is higher than non bond cut-off radius used in this calculation. Ten layers of iron atoms provide sufficient depth to overcome the issues related to cut-off radius in this case. After constructing the initial geometry of the surface and inhibitor molecules, geometry optimization is done in order to get rid of the unfavourable structures and minimize the energy of the initial geometries. Following the geometry optimization step, the inhibitor molecule is placed on Fe (1 1 0) surface and simulation was done by COMPASS (Condensed Phase Optimized Molecular Potentials for Atomistic Simulation Studies) force field. COMPASS force field of Accelrys Material Studio is considered for calculating the interaction forces between different atoms. COMPASS is the most authentic ab initio force field that ensures the accurate and simultaneous prediction of chemical properties for a wide range of chemical entities. In general, the parameterization procedure can be divided into two phases: ab initio parameterization and empirical optimization.[47] The MD simulation is performed at 298.0 K under canonical ensemble (NVT) using a time step of 1.0 fs and a simulation time of 50 ps.

The interaction energy as well as binding energy between the inhibitor molecules and Fe (1 1 0) surface are calculated by Eq. (6) and Eq. (7)[39]

$$E_{\text{interaction}} = E_{\text{total}} - (E_{\text{surface}} + E_{\text{inhibitor}}) \quad (6)$$

Herein, the total energy of the surface and inhibitor molecule is designated as E_{total}, E_{surface} is the surface energy without inhibitor and $E_{\text{inhibitor}}$ is the energy of the adsorbed inhibitor on the surface. The binding energy of the inhibitor molecule is expressed as follows.[48]

$$E_{\text{binding}} = -E_{\text{interaction}} \quad (7)$$

Results and discussions

Potentiodynamic polarization measurements

Potentiodynamic Polarization measurements are carried out to obtain the information regarding the kinetics of anodic and cathodic reaction on mild steel surface. For mild steel, at 27^0C the polarization curves in 1 M HCl solution in presence and absence of inhibitors having 5mM concentration are shown in Fig. 2. Details descriptions of similar results for individual inhibitor molecule in various concentrations are included in supplementary section (Fig. S7). Table 1 contains all the electrochemicals corrosion kinetic parameters such as corrosion potential (E_{corr}), cathodic Tafel slope (β_c), anodic Tafel slope (β_a) and corrosion current density (i_{corr}) obtained from the extrapolation of Tafel lines. The degree of surface coverage (θ) and percentage of inhibition efficiencies ($\eta_{\%P}$) are calculated by using the following equations:

$$\theta = \frac{i_{\text{corr}} - i_{\text{corr(inh)}}}{i_{\text{corr}}} \quad (8)$$

$$\eta_{\%P} = \frac{i_{\text{corr}} - i_{\text{corr(inh)}}}{i_{\text{corr}}} \times 100 \quad (9)$$

Where, i_{corr} and $i_{\text{corr(inh)}}$ are the values of the corrosion current densities of uninhibited and inhibited specimens respectively. In acidic solution, two type of reaction usually occurs in corrosion reaction. One is anodic reaction and another is of cathodic type of reaction. Anodic reaction is the transfer of metal ions from the metal surface and cathodic reaction is the release of hydrogen gas. In general, the inhibitor affects either the anodic or cathodic reaction, or sometimes both. Categorically inhibitor may be anodic or cathodic type when E_{corr} value differences between the mild steel electrode with and without protective film is larger than 85mV.[49,50] Herein, the change in E_{corr} value of our synthesized inhibitors (L^1, L^2 and L^3) are beyond borderline (Table 1). Therefore, these molecules can be classified as mixed type inhibitors.[51,52] The mixed type inhibitor is such that after the addition of inhibitors in acidic media it reduces the anodic dissolution of mild steel as well as also retards the cathodic hydrogen evolution reaction. It is also seen from Table 1 that the difference between cathodic Tafel slope (β_c) and anodic Tafel slope (β_a) are not that much higher, which further indicate that, these inhibitors control both way. Moreover, the negative shift of E_{corr} values can be successfully explained by the fact that these inhibitors produce more beneficial effect on the H^+ ion reduction (cathodic type) than that of mild steel dissolution (anodic type) reaction. Therefore, formation of protective film on the mild steel surface suppress the transfer of H^+ ion to the cathodic site of mild steel surface and thereby decreasing the rate of H_2 gas evolution. Therefore, it is now reasonable to say that these molecules behave as a mixed type inhibitors with predominately cathodic inhibitors.

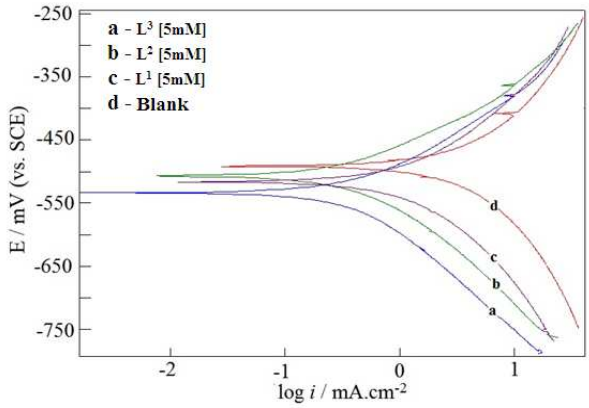

Fig. 2 Potentiodynamic polarization curves for mild steel in 1M HCl in absence and presence of Schiff bases (L^1, L^2 and L^3) having 5mM concentration.

From Table 1, it is clearly observed that corrosion current densities in the presence of inhibitors are lower compare to uninhibited solution and the corrosion current density irrespective of inhibitor concentration are decreased in the order of $L^3 > L^2 > L^1$. This result suggests that L^3 produces more beneficial effect in the corrosion inhibition process on iron surface at 1 M HCl medium. It means that $-NO_2$ substituted Schiff base has better protection ability than the

–Cl substituted derivative and subsequently un-substituted Schiff base is the least inhibitor.

Electrochemical impedance spectroscopy (EIS)

The corrosion of mild steel surface in absence and presence of inhibitors with varying concentrations in 1 M HCl solution is investigated by electrochemical impedance spectroscopy. For mild steel, Nyquist plots and Bode diagrams obtained from EIS in absence and presence of three inhibitors (*e.g.;* L^1, L^2 and L^3) in 5mM concentration are shown in Fig. 3a and 3b, while overlayed Nyquist plots for all three inhibitors in different other concentrations are shown in the supplementary section (Fig. S8). EIS spectra in absence of inhibitors merely present only one semicircle in Nyquist plot and one time constant and one negative fluctuation in bode diagram, represents the corrosion on mild steel surface in absence of Schiff base inhibitors is controlled by a charge transfer process.[53-54] In Nyquist plot, the charge transfer resistance usually stands by difference in lower and higher frequencies in real impedance. This resistance is actually corresponds in line with the resistance in between metal and outer Helmholtz plane.[55-57] Therefore the contribution of resistances in metal/solution interface is coming due to R_{ct} along with diffuse layer resistance (R_d) and accumulation resistance (R_a) have to be taken into account. Therefore the real impedance in this study at lower and higher frequencies is considered as a polarisation resistance (R_p).[55-59]

The impedance responses of mild steel after the addition of Schiff bases (L^1, L^2 and L^3) in 1 M HCl medium with increasing inhibitor concentration shows that the diameter of capacitive loops are also concomitantly increased. As observed from Fig. 3a there is an increase in values of R_p with increase in inhibitor concentration. This observation can be explained in line of the creation of a protective over layer on the metal surface. Therefore on further addition of inhibitors in the aggressive HCl medium we have to furthermore consider film resistance (R_f) in R_p.

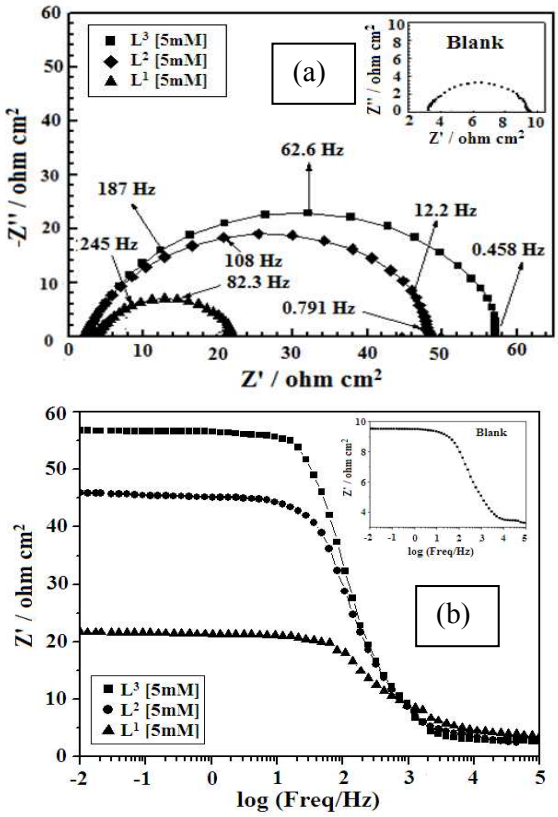

Fig. 3 (a) Nyquist plots (b) Bode diagrams in mild steel in 1 M HCl in presence of Schiff bases (L^1, L^2 and L^3) having 5mM concentration. [Inset: Nyquist plot and Bode diagram in absence of inhibitors (blank)]

Table 2 Electrochemical parameters obtained from measurements of EIS for mild steel corrosion in 1 M HCl solution in various concentrations of Schiff base inhibitors at 27^0C

System	Conc (mM)	R_s (Ω cm^2)	R_p (Ω cm^2)	Q ($\mu\Omega^{-1}s^n$ cm^{-2})	n	C_{dl} (μF cm^{-2})	$\eta_{\%Z}$	θ
HCl	Blank	3.30	6.23	593	0.818	171	—	—
L^1	0.1	3.52	8.4	751	0.77	165	25	0.25
	0.5	3.48	11.3	402	0.85	155	44	0.44
	1	3.62	12.6	499	0.807	148	51	0.51
	5	3.62	18.1	320	0.842	122	65	0.65
L^2	0.1	3.52	15.9	404	0.822	135	60	0.60
	0.5	3.66	22.7	346	0.817	117	72	0.72
	1	2.41	28	203	0.851	82.1	77	0.77
	5	2.42	43.5	97.1	0.871	43.2	85	0.85
L^3	0.1	3.52	16.7	413	0.812	130	63	0.63
	0.5	2.81	26	306	0.799	90.7	76	0.76
	1	2.28	30.1	110	0.863	44.4	79	0.79
	5	2.74	54	97	0.864	42.4	88	0.88

So R_p in presence of inhibitor can be designated as $\Sigma R_{ct}+R_d+R_a+R_f$.[55] Therefore the diameter of the Nyquist plots includes charge transfer resistance, double layer resistance, film resistance and other accumulations at metal/solution interface. Closer inspection of these plots have revealed that capacitive loops are depressed with their centre under the real axis, which is possibly due to the frequency dispersion, roughness as well as the inhomogeneities of the metal surface.[60-62] Keeping this fact in our mind, we have introduced constant phase element in the circuit to get more accurate fit. The observed Nyquist plots are analysed by fitting with an equivalent circuit containing a parallel combination of constant phase element (CPE) with the polarization resistance (R_P) as depicted in Fig. 4. R_s correspond to the solution resistant.

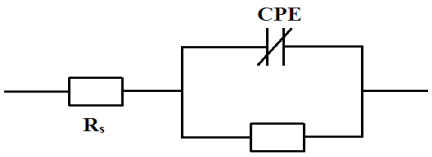

$R_p = R_{ct} + R_d + R_a$ (In absence of inhibitor)
$R_p = R_{ct} + R_d + R_a + R_f$ (In presence of inhibitor)

Fig. 4 Electrical equivalent circuit used to fit the impedance data on mild steel/solution interface in the absence and presence of inhibitors.

The constant phase element have correlation with the double layer capacity and subsequently their impedance is given by the following equation:[63-66]

$$Z_{CPE} = Q^{-1}(i\omega)^{-n} \quad (10)$$

Where Q stands for proportionality coefficient, the imaginary unit is i, ω represents angular frequency and n is a measure of irregularity on surface. Herein, CPE embodies resistance for $n = 0$, a capacitance at $n = 1$ and inductance for $n = -1$. Goodness of fit is assessed from the χ^2 values, which lies in the range of 10^{-4} to 10^{-5}. The fitted parameters obtained following the above model is given in Table 2.

A correlation between the charge transfer resistance (R_p) and double layer capacitance (C_{dl}) are calculated as follows:[65,66]

$$C_{dl} = (Q.R_p^{1-n})^{1/n} \quad (11)$$

In EIS, degree of difficulty in corrosion reaction is reflected by R_p values, higher the value of R_p lower is the corrosion rate. Inspection of EIS data in Table 2 shows that R_p value increases with increasing the concentration of Schiff bases. This reflects that these inhibitors prevent corrosion effectively and a protective layer on the electrode surface is formed. This layer acts as a barrier towards mass and charge transfer. Additionally, C_{dl} value also decreases with increasing concentration of inhibitors, which can be described by the decrease of local dielectric constant or by an increase in the thickness of electrical double layer. These results suggest that inhibitor molecules adsorb on the metal/solution interface by the replacement of water molecule and there by retards metallic dissolution.[67]

The inhibition efficiencies value can be calculated according to the following equation:

$$\eta_{\%z} = \frac{R_p - R_p^0}{R_p} \times 100 \quad (12)$$

Where, R_p^0 and R_p are the polarization resistance in absence and presence of an inhibitor molecule. The order of inhibition efficiency are following the order of $L^3 > L^2 > L^1$. This result is in well agreement with those obtained from the potentiodynamic polarization measurements. It also strengthen that $-NO_2$ group provides better adsorption potentiality for L^3, compare to L^2 (a –Cl substituted inhibitors). Latter on it is further counter supported and clearly explained in light of the results obtained from quantum chemical calculations and molecular dynamics simulations.

Adsorption isotherm

Adsorption isotherm provides the nature of interaction involves between the inhibitor molecule and metal surface. There are several kind of adsorption isotherm are present to evaluate adsorption phenomenon on the metal surface (*e.g.;* Langmuir, Temkin and Frumkin isotherms *etc.*). Experimental values obtained from EIS are investigated graphically for fitting several kinds of adsorption isotherm. Among the above isotherms, excellent fitting of the experimental values has been observed by the simplest Langmuir adsorption isotherm model. According to the Langmuir adsorption isotherm, the degree of surface coverage θ is related to the concentration of the inhibitor (C) by the following equation:[68,69]

$$C/\theta = 1/K_{ads} + C \quad (13)$$

Where, 'K_{ads}' stands for equilibrium constant in the adsorption process. A linear relationship between C/θ *Vs* C (Fig. S9) has been observed with a strong correlation coefficients (R^2) of 0.99913 for L^1, 0.99969 for L^2 and 0.99960 for L^3, respectively. Adsorption of inhibitor molecules on the adsorbent is of monolayer in nature is confirmed from Langmuir adsorption.

There is a good correlation between adsorption equilibrium constant (K_{ads}) and standard free energy of adsorption (ΔG^0_{ads}) which is as follows:

$$K_{ads} = \frac{1}{55.5}\exp\left(\frac{-\Delta G^0_{ads}}{RT}\right) \quad (14)$$

Where, R is universal gas constant and the absolute temperature is denoted by T. The molar concentration of water is expressed in mol/L and in solution its value is 55.5. The calculated thermodynamic parameters are tabulated in Table 3. In general, when ΔG^0_{ads} values is in the order of -20 kJ mol^{-1} or even lower (more positive) are consistent in proving spontaneous adsorption at the interface of charged organic molecules and charged metal surface (physisorption type).[70] On the other hand, ΔG^0_{ads} value around -40 kJ mol^{-1} or higher (more negative) involves charge transfer or sharing of it from the organic inhibitors to the iron surface *via* coordinate bond formation (chemisorptions type).[70] The corresponding ΔG^0_{ads} values for all the synthesized inhibitors are residing in the order of -30.00 to -33.50 kJ mol^{-1}. Observed range of free energies suggests adsorption on Fe-metal surface is of mixed type, which means physisorption along with chemisorption occurs in 1 M HCl medium on the mild steel surface. It is also interesting to see that when H atom in L^1 molecule is replaced by the –Cl atom forming L^2, free energy of adsorption value is increased which signifies that lone pair of chlorine atom participates in chemisorption process. When –Cl atom is replaced by the $-NO_2$ group forming L^3 free energy of adsorption value is further more increased too some extent, it reflects nitro group (a combination of one N atom and two O atom) has better chemisorption ability compare to chloride due to the three hetero atom together.

Therefore, more is the donating site better will be the adsorption of the inhibitor molecule on the metallic surface is observed. The enhancements in the absolute values of ΔG^0_{ads} are similar to the order of the inhibition efficiency obtained by potentiodynamic polarization as well as by electrochemical impedance spectroscopy.

Table 3 Thermodynamics parameters obtained from Langmuir adsorption isotherm for studied Schiff bases at 27^{0}C

Inhibitors	K_{ads} (M^{-1})	$-\Delta G_{ads}$ (kJ mol^{-1})	R^2
L^1	2.66×10^3	30.00	0.99913
L^2	10.08×10^3	33.35	0.99969
L^3	10.68×10^3	33.50	0.99960

Weight loss measurement

Inhibition efficiency obtained from weight loss measurement is very useful due its good reliability. The weight loss measurement shows that $\eta_{\%w}$ increases with increasing immersion time for all the inhibitors and attain a maximum value of 60% for L^1, 82% for L^2 and 83% for L^3. It is also seen (*vide* Fig. S10) that for the whole time range $\eta_{\%w}$ for L^1 is lower than that of L^2 and L^2 is lower than that of L^3. Increasing inhibition efficiency with increasing immersion time is due to the extent of surface coverage by the inhibitor molecules and thereby a thick protective layer on the mild steel surface is formed with time which is possibly due to physisorption. Physisorption in these inhibitors may be attributed due to weak vander waals' interactions.[71] However performance of these Schiff base molecules as promising corrosion inhibitors for mild steel in 1M HCl can also be considered in view of availability of lone pair of electrons on N, O like hetero atoms, pi electron clouds in benzene rings as well as presence of azomethine groups (–C=N) in present inhibitor molecules.[72] Therefore these inhibitors will make them susceptible for donor-acceptor (D-A) interactions in between mild steel surface with that of inhibitors. More interestingly, presence of chloro and nitro groups in L^2 and L^3 inhibitor will make them more prone towards D-A interactions which in turn reflects their better inhibition efficiency compare to L^1. This is further more supported by quantum chemical calculations (vide infra, Quantum chemical calculation). In this present study, reproducibility of the results obtained for $\eta_{\%w}$ is very precise from triplicate determination (within a range of ± 2%). Higher inhibition efficiency is maintained for 96 hours confirms robustness of inhibitors in 1 M HCl medium.

Surface analysis

Scanning Electron Microscopy (SEM) is used to examine the effectiveness of inhibitors on the corrosion process. SEM micrographs are shown in Fig. 5, where mild steel specimens are immersed for 6 h duration in 1 M HCl solution of inhibitors. Fig. 5a clearly revealed that in absence of inhibitors mild steel surface is strongly damaged due to the metal dissolution in aggressive acid medium. Therefore, large number of cracks and pits are observed over the metal surface. However it is clearly noticed that in presence of Schiff base inhibitors [Fig. 5(b-d)] relatively clean and smooth surfaces are observed. It is also observed that the rough, cracked, corroded steel surfaces displaces much better and smoother surfaces in the presence of L^2 and L^3 inhibitors. The surface smoothness of inhibited metal planes is due to formation of protective layer over the mild steel surface and this protective layer is responsible for corrosion inhibition.

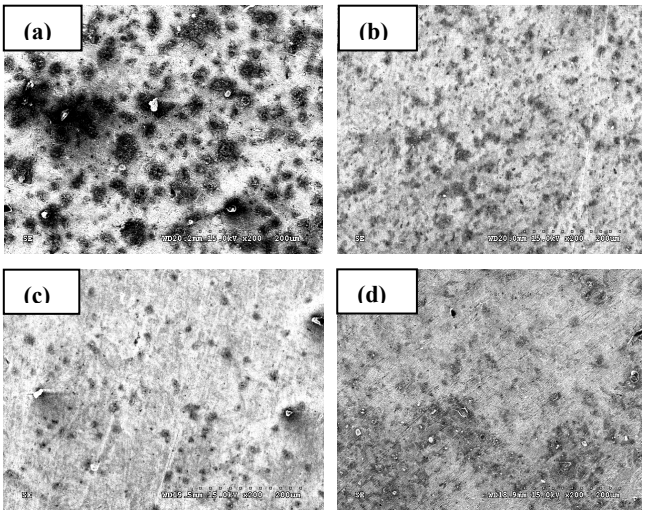

Fig. 5 SEM images of mild steel after immersion in 1 M HCl medium with (a) no inhibitor, (b) 5mM L^1, (c) 5mM L^2, (d) 5mM L^3 (magnification, ×200).

Quantum chemical calculations

Adsorption of the inhibitor molecules on the metallic surface occurs by the donation or acceptance of electrons in between the organic inhibitor and vacant d-orbitals of the metallic atom surface. The adsorption of the inhibitor molecules on the metals are related to FMOs (frontier molecular orbital energies). FMOs are of two types; highest occupied molecular orbital (HOMO) and lowest unoccupied molecular orbital (LUMO).[73,74] The energy of the E_{HOMO} is related to the electron donation capability of the respective molecule. Higher the E_{HOMO} value, stronger will be the electron donating capability of inhibitor and better will be the inhibition efficiency. E_{LUMO} indicates concerned molecules ability to accept electrons from the metallic surface. Therefore lower the E_{LUMO} value, better will be its inhibition efficiency.[75] It was observed with concomitant increase in HOMO energy and decrease in LUMO energy the binding ability of the inhibitor on the metallic surface increases. Accordingly, the energy gap between HOMO and LUMO energy level ($\Delta E = E_{LUMO}$-E_{HOMO}) is an important parameter in determining adsorption of inhibitor on metallic surface. In this regard, several quantum chemical parameters have been calculated and summarized in Table 4. Optimised geometric structures as well as frontier molecular orbital electron densities are presented in Fig. 6.

From Table 4, it could be seen that E_{LUMO} values of the three selected inhibitor remarkably decrease in the order of $L^1 > L^2 > L^3$, that means the ability to accept electrons from metallic surface obeys the order $L^3 > L^2 > L^1$. At the same time, ΔE values also decreases in the order of $L^1 > L^2 > L^3$. These are in well accordance with the result obtained from the experimental work. However, inspection of Table 4 shows that only slight difference in E_{HOMO} values are there for the inhibitors, indicating that electron donating ability of these molecules are nearly similar. This is further confirmed by calculating fraction of electron (ΔN) transferred from inhibitor to the Fe-surface. Electron affinity (A) and ionization potential (I) of inhibitors are calculated by Koopmans' theorem.[76] According to this theorem the ionization potential is related to the HOMO energy whereas electron affinity is related to the LUMO energy of the molecules respectively. Although there is no formal authentication is present within DFT concerning it, however validity of it is accepted in long run. The calculated ionization potential and electron affinity findings are used to obtain (χ) and (η) of the concerned inhibitors. These parameters have correlation with ionization potential and electron affinity as follows:

$$\chi = \frac{I + A}{2} \quad (15)$$

The global hardness (η):

$$\eta = \frac{I - A}{2} \quad (16)$$

E_{HOMO} and E_{LUMO} have correlation with I and A:

$$I = -E_{HOMO} \quad (17)$$

$$A = -E_{LUMO} \quad (18)$$

Pearson method is helpful in calculating the fraction of electrons (ΔN) transferred from inhibitor to metallic surface.[77]

Inhibitors	E_{HOMO} (eV)	E_{LUMO} (eV)	ΔE (eV)	$I = -E_{HOMO}$	$A = -E_{LUMO}$	χ (eV)	η (eV)	S (eV^{-1})	ΔN
L^1	-6.0003	-2.0486	3.9517	6.0003	2.0486	4.0244	1.9758	0.5061	0.7529
L^2	-6.0535	-2.1931	3.8604	6.0535	2.1931	4.1233	1.9302	0.5180	0.7451
L^3	-6.1954	-2.8108	3.3846	6.1954	2.8108	4.5031	1.6923	0.5909	0.7377

Table 4 Quantum chemical properties of Schiff base inhibitors

Electronegativity difference between metallic surface and inhibitors are responsible for subsequent electron transfer. In general, the electron flow is used to happen from molecule with low electronegativity to the direction of higher electronegativity side until and unless the chemical potentials will be the same. Following Pearson's idea, to find out fraction of electron transferred, a theoretical value for the absolute electronegativity of iron is considered $\chi_{Fe} = 7eV$[77] and $\eta_{Fe} = 0$, by considering for metallic bulk $I = A$[78], as because of their softer nature than neutral metallic atoms. Following the relation, we can easily calculate out ΔN to the metallic surface:

$$\Delta N = \frac{\chi_{Fe} - \chi_{inh}}{2(\eta_{Fe} + \eta_{inh})} \quad (19)$$

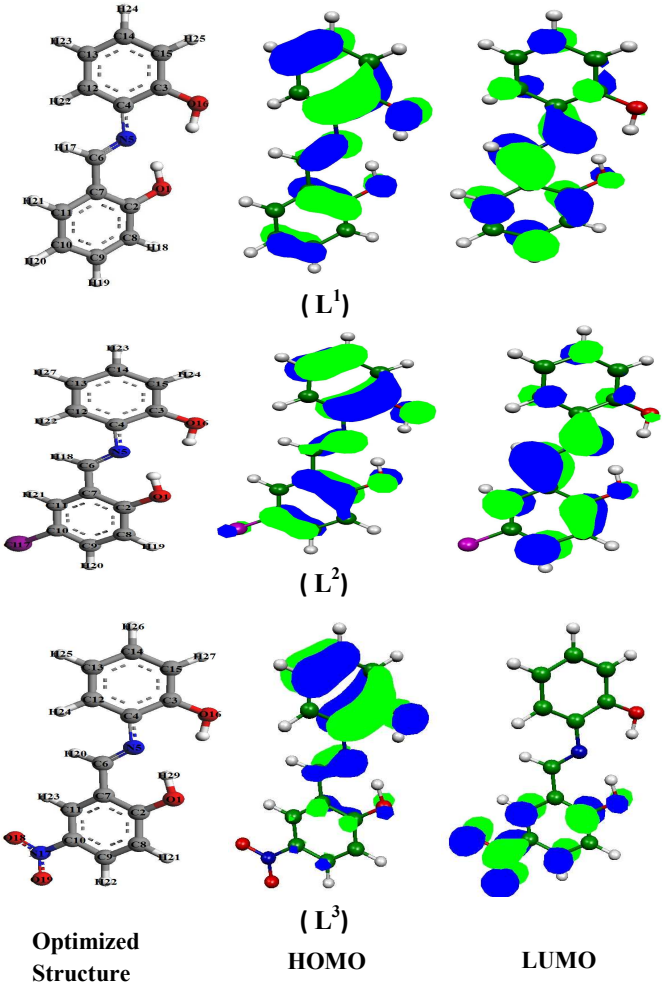

Fig. 6 DFT-derived geometry optimized structure, HOMO and LUMO plot of three Schiff base molecules at B3LYP level in aqueous phase.

Values of ΔN exhibit the electron transfer from molecule to metal surface if $\Delta N > 0$ and metal surface to molecule if $\Delta N < 0$.[79,80] According to Elnga *et al.*,[81] inhibition efficiency increases with increasing electron-donating ability of the molecule at the metal surface if $\Delta N < 3.6$. It can be concluded from Table 4 that all the values of ΔN are positive and less then 3.6, indicates that the molecules can donate its electrons to iron surface by the formation of coordinate bond. It is also observed from Table 4 that the values of ΔN of the three inhibitor molecules have only slight difference. This indicates the similar electron donating capability of the studied inhibitor molecules. Therefore after analysing the results obtained from the frontier orbital energies, we may conclude that the difference in inhibition efficiency is mainly related to the difference ability of those molecules to accept electrons from the metal surface.

On the other hand, electronegativity (χ) represent electron attracting capability of the molecule. Higher the electronegativity, stronger is the attracting power to accept electron from the metallic surface. Therefore, those inhibitor molecules which possessed higher electronegativity would have strong interaction with the metal surface and higher inhibition efficiency is observed. From Table 4, it is observed that electronegativity of the three inhibitor molecules follows the trend $L^3 > L^2 > L^1$.Therefore, it is confirmed that L^3 has the highest ability to accept electrons among the three inhibitor molecules and these results are in well agreement with the E_{LUMO} trend.

Softness is another important issue to be concerned for the studied Schiff base inhibitors on metal surface. In this study, inhibitors are considered as soft base and the metals as soft acid.[21] Thus, soft-soft interaction is the most predominant factor for the adsorption of inhibitor molecules. It is seen from Table 4, that the calculated values of softness are follows the order: $L^3 > L^2 > L^1$, which further supports the better adsorption power of L^3 on the metal surface.

Active sites

Inhibitor molecules usually donate its electrons to the metallic surface and accept electrons from the metallic surface as well; therefore it is reasonable to examine the active sites of the inhibitor molecules. To investigate the active sites of an inhibitor, three controlling factors have to be considered: (i) neutral atomic charge, (ii) distribution of frontier molecular orbitals and (iii) Fukui indices. Here, Fukui indices are used to analyse the local reactivity as well as nucleophilic and electrophilic behaviour of the studied inhibitors.[82,83] The nucleophilic and electrophilic attacks are determined by f_k^+ and f_k^-. Generally, high value of f_k^+ and f_k^- implies high capacity of the atom to accept and donate electrons, respectively. The calculated Fukui indices for the studied inhibitors are presented in Table S1. It can be seen that for L^1 molecule O(1), C(2), N(5), C(6), C(9) and C(14) atoms are the most susceptible sites for accepting electron from metallic surface as those atoms posses highest value of f_k^+, 0.047 for O(1), 0.046 for C(2), 0.085 for N(5), 0.120 for C(6), 0.073 for C(9), 0.056 for C(11) and 0.045 for C(14), respectively. On the other hand, O(1), C(3), C(4), C(13), C(14) and O(16) atoms are the preferable sites to donate electron as those are presented largest value of f_k^-, 0.055 for O(1), 0.064 for C(3), 0.064 for C(4), 0.071 for

C(13), 0.062 for C(14) and 0.084 for O(16), respectively. However in L^2, incorporation of chloro group in L^1 molecule, the distributions of active sites and their corresponding values for nucleophilic and electrophilic attacks are nearly similar, additionally Cl(17) atom has participated for electron donation and acceptance due to its larger f_k^+ (0.045) and f_k^- (0.066) values. Thus, it is concluded that presence of chloro moiety helps in enhancement of chemisorptions property of L^2 compare to L^1 which is also already confirmed from ΔG^0_{ads} value in adsorption isotherm segment. These two different domains reflects the same outcome. Similarly in L^3 where chloro group of L^2 is replaced by nitro group, the distributions of active sites are quite different than that of L^2. Here, O(1), C(2), C(9), C(11), N(17), O(18) and O(19) atoms are the preferred sites for electron acceptance whereas C(3), C(4), C(6), C(13), C(14), C(15) and O(16) atoms are responsible for electron donation. Now It can be well concluded that the nitro substituted phenyl group (LUMO of L^3 in Fig. 6) is mostly participating for accepting electrons whereas the azomethine as well as phenol segments (HOMO of L^3 in Fig. 6) are responsible for electron donation. In summary, in L^3 one part is responsible for electron donation while the other part is preferable for electron acceptance. Both the units of a single inhibitor are individually playing important roles for the adsorption process regarding adsorption process on the metallic surface as it is well known that better the adsorption property better will be the inhibition efficiency too.The HOMO, LUMO electronic distribution are in well agreement with the calculated fukui indices, where both way calculated output supports the same reactive zones for corresponding interactions on iron surface.

Molecular dynamics simulation

Recently, MD simulation has emerged as a modern tool to investigate the adsorption behavior of the inhibitor molecule on the metallic surface.[84,85] MD simulation can reasonably predict the most favorable configuration of the adsorbed inhibitor molecule on the Fe-surface. Thus for a better insightfulness in the adsorption phenomenon, all three selected inhibitors (L^1, L^2 and L^3) have been considered to act on the Fe (1 1 0) surface to determine the suitable and adorable adsorption configuration. In this context, when the temperature and energy of the system reaches in an equilibrium, $E_{interaction}$ and $E_{binding}$ between the inhibitor and Fe (1 1 0) surface can be correlated according to the Eq. (6) and Eq. (7), respectively. The calculated $E_{interaction}$ and $E_{binding}$ values are tabulated in Table 5. The best adsorption configuration of the inhibitor over Fe (1 1 0) surface as well as the close contacts between those are depicted in Fig. 7. It is clearly observed (*infra*, vide Fig. 7) that all three inhibitor molecules are adsorbed on the Fe (1 1 0) surface with almost parallel or flat dispositions. This flat orientation is possibly due to the formation of coordination and back-bonding between the inhibitor and metal surface. It is also evident herein that the presence of unoccupied metal d-orbitals will prefer to accept electron from the adsorbed inhibitor molecule. All three selected inhibitors have lone pair of electrons on the N, O and Cl like atoms as well as π-electrons in the benzene rings. Those atoms and π-electron cloud in the benzene ring provides sufficient electronic charge to the vacant d-orbitals of metal in forming of stable coordination bond. On the other hand, empty π-antibonding orbital of phenyl segment have sufficient orbital space to accomodate electrons from d-orbital of iron to form feedback bonds. Therefore inhibitors as a whole are responsible for flat or parallel orientation as well as disposition on the Fe (1 1 0) surface. This flat orientation of the inhibitor molecules with respect to the Fe surface will definitely provide larger blocking area and therefore preventing the metal surface from acid attack.

Table 5 Output obtained from MD simulation for adsorption of inhibitors on Fe (1 1 0) surface

Systems	$E_{interaction}$ (kcal/mol)	$E_{binding}$ (kcal/mol)
Fe + L^1	-120.989	120.989
Fe + L^2	-130.055	130.055
Fe + L^3	-143.492	143.492

The calculated values of interaction energies of the adsorption systems are -120.989, -130.055 and -143.492 kcal mol^{-1} for L^1, L^2 and L^3 respectively. The strong adsorption between the inhibitor and the Fe (1 1 0) surface is confirmed from the large interaction energy values.[78]

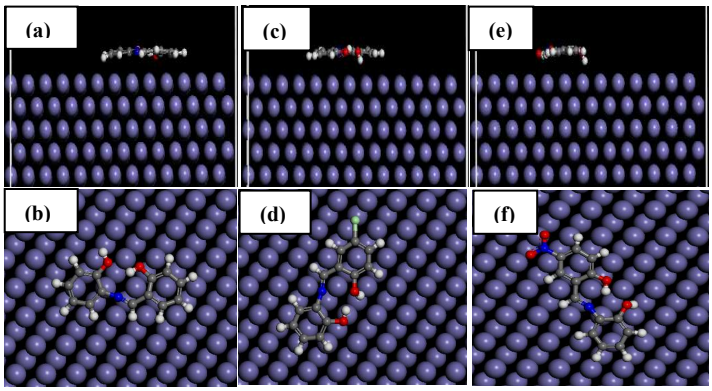

Fig. 7 Equilibrium adsorption configurations of inhibitors L^1 (a and b), L^2 (c and d) and L^3 (e and f) on Fe (1 1 0) surface obtained by MD simulations. Top: top view, Bottom: side view.

The calculated values of interaction energies during the simulation process revealed that L^3 has the highest interaction energy of the three tested inhibitors. From theoretical aspect, we may confirm that the highest interaction energy of L^3 also reflects that it has highest adsorption ability on the Fe surface. Moreover, the high magnitude of binding energy suggests a better and stable adsorption (*vide* Table 5) system with a higher inhibition efficiency.[86] Thus in conclusion it can be said from the values of interaction energy and binding energy that the stability of the inhibitor molecules on the iron surface are ranked as $L^3 > L^2 > L^1$. MD simulation results are in excellent agreement with the results coming out from quantum chemical calculations as well as from experimental findings.

Conclusions

A combined experimental and theoretical approach is employed in this present study to investigate the corrosion inhibition performance of three Schiff base molecules on mild steel surface. The following conclusions are summarized as follows:

1) Polarization study reveals that these three Schiff base molecules behave as a mixed type inhibitors with predominantly cathodic inhibitive capacity.

2) EIS measurements reveals that polarization resistance (R_p) increases at the metal-electrolyte interfaces confirming adsorption mostly occurs by these inhibitor molecules on the mild steel surface.
3) The inhibitors adsorption on Fe surface follows Langmuir adsorption profile.
4) A good correlation is found in between the quantum chemical parameters (E_{LUMO}, energy gap (ΔE), electronegativity (χ), softness (S)) and experimentally obtained inhibition efficiencies of the studied inhibitors. However, only a slight difference in E_{HOMO} and fraction of electron transfer (ΔN) values are observed. This can successfully explain that these compounds receive electrons from the metal surface which in turn reinforce the adsorption of these molecules on the metallic surface.
5) The reactive sites of the inhibitor molecules for nucleophilic and electrophilic attack are thoroughly investigated by Fukui indices.
6) The MD simulations reveals that three Schiff base molecules adsorb on the mild steel surface in the planar orientation with higher negative interaction energy and the adsorption stability decreases in the following order $L^3 > L^2 > L^1$, which is in accordance with the experimentally observed inhibition efficiency.

In summary, all these studies are in well resemblance with the results obtained from three different domains starting from wet chemical experimentation followed by quantum chemical calculation (based on quantum chemistry) and finally molecular dynamics simulation (based on classical physics). From all these successful correlation it can be concluded wet chemical experiments followed by DFT along with MD simulation can provide a perfect picture towards inhibition study and in getting the interactions between the inhibitor molecules and the metal surfaces.

Acknowledgements

Department of Science and Technology, Govt. of India sponsored Fast Track Project (vide ref. no: SB/FT/CS-003/2012 and project no: GAP-183112) is gratefully acknowledged for getting the computational infrastructure facility for carrying out the DFT and MD calculations. SS would like to acknowledge DST (GAP-121512), India for his fellowship.

Notes and references

[a]*Surface Engineering & Tribology Group, CSIR-Central Mechanical Engineering Research Institute, Mahatma Gandhi Avenue, Durgapur 713209, West Bengal, India.*

E-mail: pr_banerjee@cmeri.res.in; Fax: +91-343-2546 745; Tel: +91-343-6452220
[b]*Academy of Scientific & Innovative Research, Anusandhan Bhawan, 2 Rafi Marg, New Delhi 110001, India*
[c]*Department of Chemistry, National Institute of Technology, Durgapur 713 209, India*

†Electronic Supplementary Information (ESI) available: [FTIR, ESI-MS, Potentiodynamics polarization curves, Nyquist plots, Langmuir adsorption plots, Weight loss measurements, Fukui indices for all the molecules are included in the supplementary information]. See DOI: 10.1039/b000000x/

1 H. Keles, M. Keles, I. Dehri and O. Serindag˘, *Mater. Chem. Phys.,* 2008, **112**, 173.
2 H. Wang, H. Fan and J. Zheng, *Mater. Chem. Phy*s., 2003, **77**, 655.
3 S. A. A. El-Maksoud and A. S. Fouda, *Mater. Chem. Phys.,* 2005 **93**, 84.
4 K. F. Khaled, *J. Int. Electrochem. Sci.,* 2008, **3**, 462.
5 I. Zaafarany, *Port. Electrichem. Acta.,* 2009, **27**, 631.
6 J. Aljourani, K. Raeissi and M. A. Golozar, *Corros. Sci.,* 2009, **51**, 1836.
7 M. L. Zheludkevich, K. A. Yasakau, S. K. Poznyak and M. G. S. Ferreira, *Corros. Sci.,* 2005, **47**, 3368.
8 I. B. Obot, N. O. Obi-Egbedi and S. A. Umoren, *Corros. Sci.,* 2009, **51**, 276.
9 M. G. Hosseini, M. Ehteshamzadeh and T. Shahrabi, *Electrochim. Acta.,* 2007, **52**, 3680.
10 H. H. Hassan, E. Adbelghani and M. A. Amin, *Electrochim. Acta.,* 2007, **52**, 6359.
11 Y. Abdoud, A. Abourrriche, T. Saffaj, M. Berrada, M. Charrouf, A. Bennamara, N. Al Himidi and H. Hannache, *Mater. Chem. Phys.,* 2007, **105**, 1.
12 M. A. Quaraishi, J. Rawat and M. Ajmal, *J. Appl. Electrochem.,* 2000, **30**, 745.
13 M. Behpour, S. M. Ghoreishi, N. Soltani and M. Salavati-Niasari, *Corros. Sci.,* 2009, **51**, 1073.
14 H. Ju, Z. P. Kai and Y. Li, *Corros. Sci.,* 2008, **50**, 865.
15 H. D. Leçe, K. C. Emregül and O. Atakol, *Corros. Sci.,* 2008, **50**, 1460.
16 S. Issaadi, T. Douadi, A. Zouaoui, S. Chafaa, M. A. Khan and G. Bouet, *Corros. Sci.* 2011, **53,** 1484.
17 K. R. Ansari, M. A. Quraishi and A. Singh, *Corros. Sci.,* 2014, **79**, 5.
18 M. G. V. Satyanarayana, V. Himabindu, Y. Kalpana, M. R. Kumar and K. Kumar, *J. Mol. Struc. (Theochem),* 2009, **912**, 113.
19 T. H. Muster, A. E. Hughes, S. A. Furman, T. Harvey, N. Sherman, S. Hardin, P. Corrigan, D. Lau, F. H. Scholes, P.A. White, M. Glenn, J. Mardel, S. J. Garcia and J. M. C. Mol, *Electrochim. Acta.,* 2009, **54**, 3402.
20 Y. Yan, X. Wang, Y. Zhang, P. Wang and J. Zhang, *Molecular Simulation*, 2013, **39**, 1034.
21 I. B. Obot and Z. M. Gasem, *Corros. Sci.*, 2014, **83**, 359.
22 (a) S. K. Saha, A. Hens, A. R. Chowdhury, A. K. Lohar, N. C. Murmu and P. Banerjee, *Can. Chem. Trans.*, 2014, **2**, 489. (b) S. K. Saha, A. Hens, A. R. Chowdhury, P. Ghosh and P. Banerjee, Under Communated.
23 S. K. Saha, P. Ghosh, A. Hens, N. C. Murmu and P. Banerjee, *Physica E*, 2015, **66**, 332.
24 I. Kaya, S. Culhaoglu and D. Senol. *Chinese. J. Polym. Sci*., 2007, **25**, 461.
25 J. P. Cain, P. L. Gassman, H. Wang and A. Laskin, *Phys. Chem. Chem. Phys.,* 2010, **12**, 5206.
26 A. M. Khedr and H. M. Marwani, *Int. J. Electrochem. Sci.,* 2012, **7**, 10074.
27 M. Karnahl, S. Tschierlei, C. Kuhnt, B. Dietzek, M. Schmitt, J. Popp, M. Schwalbe, S. Krieck, H. Gorls, F. W. Heinemann and S. Rau, *Dalton Trans.*, 2010, ***39***, 2359.
28 H. A. Patwardhan, S. Gopinathan and C. Gopinathan, *Ind. J. Chem*., 1978, **16**, 224.
29 John Coates, Interpretation of Infrared Spectra, A Practical Approach, John Wiley & Sons Ltd, Chichester, 2000.
30 F. Neese, An Ab ini tio, DFT and Semiempirical SCF-MO Package, Version 2.9; Max Planck Institute for Bioinorganic Chemistry, Mulheim an der Ruhr, Germany, Jan (2012).
31 D. A. Becke, *J. Chem. Phys.*, 1986, **84,** 4524.
32 D. A. Becke, *J. Chem. Phys.*, 1993, **98,** 5648.
33 C. Lee, W. Yang and G. R. Parr, *Phys. Rev. B.*, 1988, **37,** 785.
34 P. Banerjee, A. Company, T. Weyhermuller, E. Bill and C. R. Hess, *Inorg. Chem.*, 2009, **48,** 2944.
35 P. Banerjee, S. Sproules, T. Weyhermuller, S.D George and K. Wieghardt, *Inorg. Chem.,* 2009, **48**, 5829.

36 S. Joy, T. Krämer, N. D. Paul, P. Banerjee, J. E. McGrady and S. Goswami, *Inorg. Chem.,* 2011, **50**, 9993.
37 A. Schafer, C. Huber and R. Ahlrichs, *J. Chem. Phys.*, 1994, **100**, 5829.
38 A. Schafer, H. Horn and R. Ahlrichs, *J. Chem. Phys.,* 1992, **97**, 2571.
39 Materials Studio 6.1 Manual (Accelrys, Inc., San Diego, CA, 2007).
40 Z. Cao, Y. Tang, H. Cang, J. Xu, G. Lu and W. Jing, *Corros. Sci.*, 2014, **83**, 292.
41 J. A. Ciezak and S. F. Trevino, *J. Phys. Chem. A*., 2006, **110**, 5149.
42 R. G. Parr and W. Yang, *J. Am. Chem. Soc.,* 1984, **106**, 4049.
43 F. D. Proft, J. M. L. Martin and P. Geerlings, *Chem. Phys. Lett.,* 1996, **256**, 400.
44 R. R. Contreras, P. Fuentealba, M. Galvan and P. Perez, *Chem. Phys. Lett.,* 1999, **304**, 405.
45 F. L. Hirshfeld, *Theor. Chem. Acc*., 1977, **44,** 129.
46 L. Guo, S. Zhu, S. Zhang, Q. He and W. Li, *Corros. Sci.*, 2014, **87**, 366.
47 H. Sun, *J. Phys. Chem. B.,* 1998, **102**, 7338.
48 N. A. Al-Mobarak, K. F. Khaled, M. N. H. Hamed, K. M. Abdel-Azim and N. S. Abdelshafi, *Arab. J. Chem.,* 2010, **3**, 233.
49 W. Li, Q. He, S. Zhang, C. Pei and B. Hou, *J. Appl. Electrochem.*, 2008, **38,** 289.
50 E. S Ferreira, C. Giacomelli, F. C. Giacomelli and A. Spinelli, *Mater. Chem. Phys.,* 2004, **83**, 129.
51 M. A. Hegazy, *Corros. Sci.*, 2009, **51,** 2610.
52 L. R. Chauhan and G. Gunasekaran, *Corros. Sci.*, 2007, **49,** 1143.
53 M. El Achouri, S. Kertit, H. M. Gouttaya, B. Nciri, Y. Bensouda, L. Perez, M. R. Infante and K. Elkacemi, *Prog. Org. Coat*., 2001, **43**, 267.
54 A. Chetouani, A. Aouniti, B. Hammouti, N. Benchat, T. Benhadda and S. Kertit, *Corros. Sci* , 2003, **45**, 1675.
55 R. Solmaza, G. Kardas, M. Culha, B. Yazıcı and M. Erbil *Electrochim. Acta.* 2008, **53**, 5941–5952.
56 M. O¨zcan, I˙. Dehri and M. Erbil, *Appl. Surf. Sci.*, 2004, **236**, 155–164.
57. R. Solmaz, *Corros. Sci.*, 2010, **52**, 3321–3330.
58 S. Safak, B. Duran, A. Yurt and G. Turkoglu, *Corros. Sci.*, 2012, **54**, 251.
59. R. Solmaz, G. Kardas, B. Yazıcı and M. Erbil, Colloids and Surfaces A: Physicochem. Eng. Aspects, 2008, **312**, 7–17.
60 R. Solmaz, E. Altunbas and G. Kardas, *Mater. Chem. Phys.*, 2011, **125**, 796.
61 A. Chetouani, A. Aouniti, B. Hammouti, N. Benchat, T. Benhadda and S. Kertit, *Corros. Sci.*, 2003, **45,** 1675.
62 M. Behpour, S. M. Ghoreishi, N. Soltani and M. Salavati-Niasari, *Corros. Sci.*, 2009, **51,** 1073.
63 S. John and A. Joseph, *RSC Adv.,* 2012, **2**, 9944.
64 J. B. Jorcin, M. E. Orazem, N. P´eb`ere and B. Tribollet, *Electrochim. Acta.,* 2006, **51**, 1473.
65 X. Wu, H. Ma, S. Chen, Z. Xu and A. Sui, *J. Electrochem. Soc.,* 1999, **146**, 1847.
66 M. Lebrini, F. Robert and C. Roos, *Int. J. Electrochem. Sci.,* 2010, **5**, 1698.
67 X. Wang, H. Yang and F. Wang, *Corros. Sci.*, 2011, **53**, 113.
68 P. Roy, A. Pal and D. Sukul, *RSC Adv.,* 2014, **4**, 10607.
69 P. Roy, P. Karfa, U. Adhikari and D. Sukul, *Corros. Sci.*, 2014, **88**, 246.
70 S. Issaadi, T. Douadi, A. Zouaoui, S. Chafaa, M. A. Khan and G. Bouet, *Corros. Sci.*, 2011, **53,** 1484.
71 D. Kesavan, M. M. Tamizh, M. Gopiraman, N. Sulochana and R. Karvembu, *J. Surfact. Deterg.,* 2012, **15**, 567.
72 K. F. Khaled, *Appl. Surf. Sci.*, 2010, **256**, 6753–6763.
73 A. Ehsani, M. G. Mahjani, R. Moshrefi, H. Mostaanzadeh and J.S. Shayeh, *RSC adv.,* 2014, **4**, 20031.
74 S. K. Saha, P. Ghosh, A. R. Chowdhury, P. Samanta, N. C. Murmu, A. K. Lohar and P. Banerjee, *Can. Chem. Trans.,* 2014, **2**, 381.
75 K. F. Khaled, *Appl. Surf. Sci.*, 2008, **255**, 1811.
76 I. Lukovits, E. Kalman and F. Zucchi, *Corrosion*, 2001, **57,** 3.
77 S. Martinez, *Mater. Chem. Phys.*, 2002, **77**, 97.
78 M. J. S Dewar and W. Thiel, *J. Am. Chem. Soc.*, 1977, **99**, 4899.
79 A. Kokalj, *Electrochim. Acta,* 2010, **56**, 745.
80 N. Kovac˘evic´ and A. Kokalj, *Corros. Sci.*, 2011, **53**, 909.
81 M. K. Awad, M. R. Mustafa and M. M. A. Elnga, *J. Mole. Struct. (Theochem).,* 2010, **959**, 66.
82 S. John, M. Kuruvilla and A. Joseph, *RSC adv.,* 2013, **3**, 8929.
83 N. O. Obi-Egbedi and I. B. Obot, *Corros. Sci.,* 2011, **53**, 263.
84 F. Zhang, Y. Tang, Z. Cao, W. Jing, Z. Wua and Y. Chen, *Corros. Sci.,* 2012, **61**, 1.
85 A. Y. Musa, A. A. H. Kadhum, A. B. Mohamad and M. S. Takriff, *Corros. Sci.*, 2010, **52,** 3331.
86 K. F. Khaled, *J. Appl. Electrochem.*, 2011, **41**, 423.